

R. Wenninger, T.H. Eich, G.T.A. Huysmans, P.T. Lang, S. Devaux,
S. Jachmich, F. Köchl and JET EFDA contributors

Scrape Off Layer Heat Transport and Divertor Power Deposition of Pellet Induced ELMs

Scrape Off Layer Heat Transport and Divertor Power Deposition of Pellet Induced ELMs

R. Wenninger¹, T.H. Eich², G.T.A. Huysmans³, P.T. Lang², S. Devaux²,
S. Jachmich⁴, F. Köchl⁵ and JET EFDA contributors*

JET-EFDA, Culham Science Centre, OX14 3DB, Abingdon, UK

¹*Universitätssternwarte der Ludwig-Maximilians-Universität, 81679 München, Germany*

²*Max-Planck-Institut für Plasmaphysik, EURATOM Association, Garching, Germany*

³*CEA Cadarache, Association Euratom/CEA, 13108, St Paul-Lez-Durance, France*

⁴*Laboratory for Plasma Physics, Ecole Royal Militaire/Koninklijke Militaire School,
B-1000 Brussels, Belgium*

⁵*Association EURATOM-ÖAW, Atominstitut, TU Wien, 1020 Wien, Austria*

** See annex of F. Romanelli et al, "Overview of JET Results",
(23rd IAEA Fusion Energy Conference, Daejeon, Republic of Korea (2010)).*

Preprint of Paper to be submitted for publication in Proceedings of the
38th EPS Conference on Plasma Physics
Strasbourg, France
(27th June 2011 - 1st July 2011)

“This document is intended for publication in the open literature. It is made available on the understanding that it may not be further circulated and extracts or references may not be published prior to publication of the original when applicable, or without the consent of the Publications Officer, EFDA, Culham Science Centre, Abingdon, Oxon, OX14 3DB, UK.”

“Enquiries about Copyright and reproduction should be addressed to the Publications Officer, EFDA, Culham Science Centre, Abingdon, Oxon, OX14 3DB, UK.”

The contents of this preprint and all other JET EFDA Preprints and Conference Papers are available to view online free at www.iop.org/Jet. This site has full search facilities and e-mail alert options. The diagrams contained within the PDFs on this site are hyperlinked from the year 1996 onwards.

INTRODUCTION

It is currently assumed that a reliable control technique for ELMs is mandatory for the success of ITER to meet restrictions in power loads to the target [1, 2, 3]. In view of next step fusion devices it is of paramount importance to reach some level of understanding in the process of inducing ELMs by pellets. Due to the technically given toroidal asymmetric nature of pellet injection the question arises, if the spatial structure of the perturbation associated with pellet induced ELMs features a corresponding toroidal asymmetry in the SOL and in the divertor. The paper recapitulates the finding of a toroidal asymmetric divertor deposition pattern during pellet induced ELMs employing a new JET divertor infrared system and compares these to nonlinear simulations.

1. EXPERIMENTAL OBSERVATIONS

Divertor InfraRed tomography (IR) in combination with magnetic field line tracing has previously been employed to investigate the structure of spontaneous ELMs [3]. We apply this method in conjunction with a ramp of the toroidal magnetic field (2.2T to 2.8T, q_{95} 4.8 to 3.6) in order to manipulate the position of the divertor imprint of a (transient) toroidally localised filament. Some key parameters of the discharge analyzed in this paper (Pulse No: 79573) are: $I_p = 20\text{MA}$, $P_{\text{NBI}} \approx 8\text{MW}$ and $\delta = 0.27$ (low triangularity). Figure 1a displays the evolution of a number of further parameters. Pellets of a nominal particle content of 2×10^{21} ($\sim 30\times$ trigger threshold [4]) have been injected perpendicularly from the magnetic low field side mid plane at 4Hz with velocities between 170m/s and 200m/s.

As already shown in [5] significant differences according to the divertor deposition structure have been observed during spontaneous and pellet induced ELMs. Figure 1b shows the radial target position of the largest peaks of the divertor power flux density proles defined by a threshold criterion versus $|B_T|$. The threshold criterion is fulfilled when the local power flux density exceeds 85% of the maximum power flux density within the prole during an investigated period ($t = 0$ to $t = 0.4\text{ms}$ with $t = 0$ defined by the peak power deposition). One can see that the locations of most peaks associated with pellet induced ELMs show a clear correlation with $|B_T|$, while spontaneous ELMs have peaks scattering around the same location for all values of $|B_T|$.

A comparative analysis of various divertor power load aspects has been carried out [5, 6]. Here spontaneous and pellet induced ELMs chosen on the basis of selection criteria described in [6] have been analyzed. A maximum power flux density on the outer target during the entire ELM of $23 \pm 5\text{MW m}^2$ for spontaneous and $30 \pm 7\text{MW m}^2$ for pellet induced ELMs has been found.

2. CODE PREDICTIONS FROM JOREK

The non-linear MHD code JOREK [7] evolves a set of reduced MHD equations in 3D. The computational domain includes the plasma center, the separatrix, the x-point and the open field lines in the SOL. For the simulation of pellet induced ELMs a JET-like H-mode plasma [8] has been chosen with an pedestal pressure gradient such that the plasma is marginally stable with respect to low to medium-n ballooning modes. In the simulations the pellet is described by a large local

particle source located in the middle of the pedestal at the magnetic low field side with a half-width of 2cm and acting adiabatically on the plasma.

Figure 2a) shows a contour of the density as well as the temperature on the separatrix and the heat flux convected to the target ~ 50 ms after the start of the pellet source. A helical perturbation with the dominant toroidal mode number $n = 1$ can be observed. At this time the pressure in the pellet cloud at the mid plane is about twice the pressure at the top of the pedestal and remains relatively constant. Figure 2b) shows a close-up of the density prole at the toroidal angle where the pellet cloud is passing the x-point. Here as well the contours of the electrostatic potential ($E \times B$ ow lines) from the JOREK calculation are illustrated. From the high density region of the helical pellet cloud there is an $E \times B$ ow across the separatrix close to the x-point directed towards the divertor. This $E \times B$ ow is found by the model to be clearly stronger towards the outer divertor leg, which is the one with the higher simulated power flux densities on the divertor.

The $E \times B$ ow leads to prompt losses of particles close to the x-point. Since the particles crossing the separatrix have been heated by parallel transport inside the separatrix, we expect that there is also an associated convected heat transport. After the separatrix crossing the parallel transport might have a more dominant role.

Figure 3a) illustrates the power flux density on the outer divertor calculated by JOREK for a time ~ 40 ms after the onset of the particle source as a function of radial divertor position R_{div} and toroidal angle Φ . At a radial position of 3.25m there is high or even maximum deposition for all toroidal angles. This position corresponds to the separatrix mapped on the outer divertor target. In addition to this symmetric deposition component another component changing maximum power flux density and prole shape with the toroidal angle can be observed. This component is spreading toroidally towards a symmetric shape with approximately the local sound speed in the x-point region.

In order to isolate the asymmetric component we identify the toroidal angle, for which the power flux density integrated along the radial direction is minimum (Fig.3c). We select the radial power flux density prole for this toroidal angle as the prole, which describes in the best way the symmetric component. We subtract this prole of the power flux density proles for each toroidal angle and obtain the proles of the asymmetric component, which are shown in figure 3b). Figure 3d) illustrates the proles for the toroidal position with the maximum asymmetric contribution.

The maximum power flux density of the total deposition evaluated for each toroidal position has a maximum variation of 66% of the mean value, which is a much larger variation than the experiment describes. Thus a considerable toroidal asymmetry in the maximum power flux density is predicted by JOREK. Figure 3d) indicates the location of the maximum power flux density for all toroidal locations for the total deposition and the asymmetric component. In real space coordinates the line for the total deposition would appear as a structure similar to a spiral.

By means of JOREK calculations and SOL field line tracing a number of indications regarding the nature of the toroidally asymmetric component of the transport associated with pellet induced ELMs has been gathered. As further discussed in [5] there are two candidate positions for the separatrix crossing: a) X-point region and b) pellet injection location.

SUMMARY

We recall that the ultimate goal of inducing ELMs by pellets is the reduction of the deteriorating effect of the ELMs on the plasma facing components [9]. In the light of this the striking feature of pellet induced ELMs to cause an asymmetric divertor power load deserves particular attention. In the simulation the toroidal variation of the maximum power flux density is 66% for the total deposition. In qualitative comparison the experiment with asymmetric component in the IR-view the peak heat flux of pellet induced ELMs is found to be considerably larger than for spontaneous ELMs. It is not clear, if the asymmetric component is of similar extent for ELMs induced by pellets injected from the high field side, or ELMs induced by smaller pellets and how it scales with major radius. Consequently it can not be excluded that pellet injection at fixed q_{95} in next step fusion devices such as ITER causes considerable toroidally localised enhanced divertor degradation.

REFERENCES

- [1]. Federici G. et al 2003, Journal of Nuclear Materials **313-316** 11-22
- [2]. Loarte A. et al 2003, Journal of Nuclear Materials **313-316** 962-966
- [3]. Eich T. et al 2005, Journal of Nuclear Materials **337-339** 669-676
- [4]. Lang P. et al 2011, Nuclear Fusion **51** 1-16
- [5]. Wenninger R.P. et al 2010, 37th EPS Conf. on Controlled Fusion and Plasma Physics
- [6]. Wenninger R.P. et al 2011, Submitted to Plasma Physics and Controlled Fusion
- [7]. Huysmans G.T.A et al 2009, Plasma Physics and Controlled Fusion **51** 124012
- [8]. Huysmans G.T.A et al 2010, 37th EPS Conf. on Controlled Fusion and Plasma Physics
- [9]. Lang P. et al 2004, Nuclear Fusion **44** 665-677

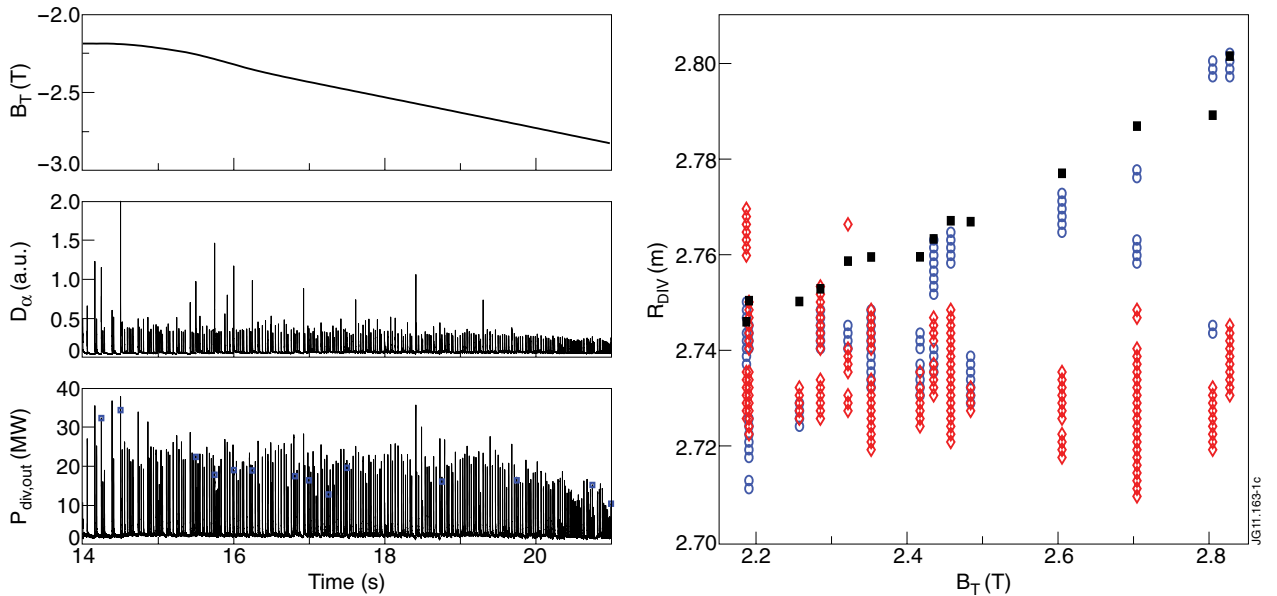


Figure 1: a) Time traces of toroidal magnetic field, D_α -radiation, power to the outer target, edge line integrated density and pellet monitor signal. b) Observed peak positions (criterion is described in the text) for pellet induced ELMs (blue dots) and spontaneous ELMs (red dots) as function of $|B_T|$ Pulse No: 79573 (Fuelling size pellets / LFS): Squares indicate predicted and corrected peak positions on the basis of field line tracing with $\Phi_{mp} = \Phi_{pel}$.

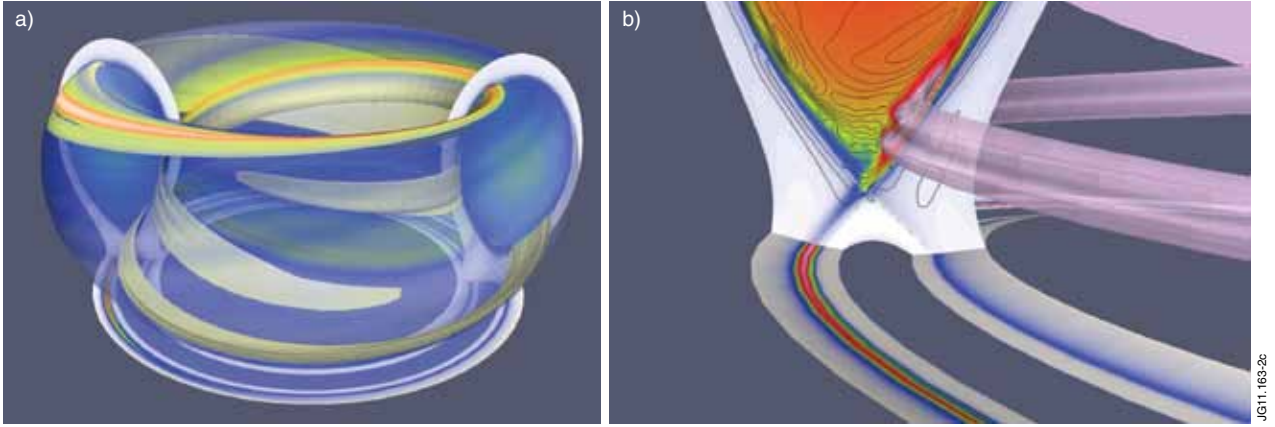


Figure 2: a) The density contour ($n = 1.1 \times n_{mag}$ axis) at $t \sim 50\text{ms}$, the temperature at the separatrix (red-blue scale) and the convected heat flux to the target. The pellet injection location is on the LFS mid plane on the side of the plasma, which is turned away from the viewer. b) Close-up of the density contour together with the contours of the electrostatic potential ($E \times B$ flow lines, black contours). The heat convected to the target is illustrated in both figures.

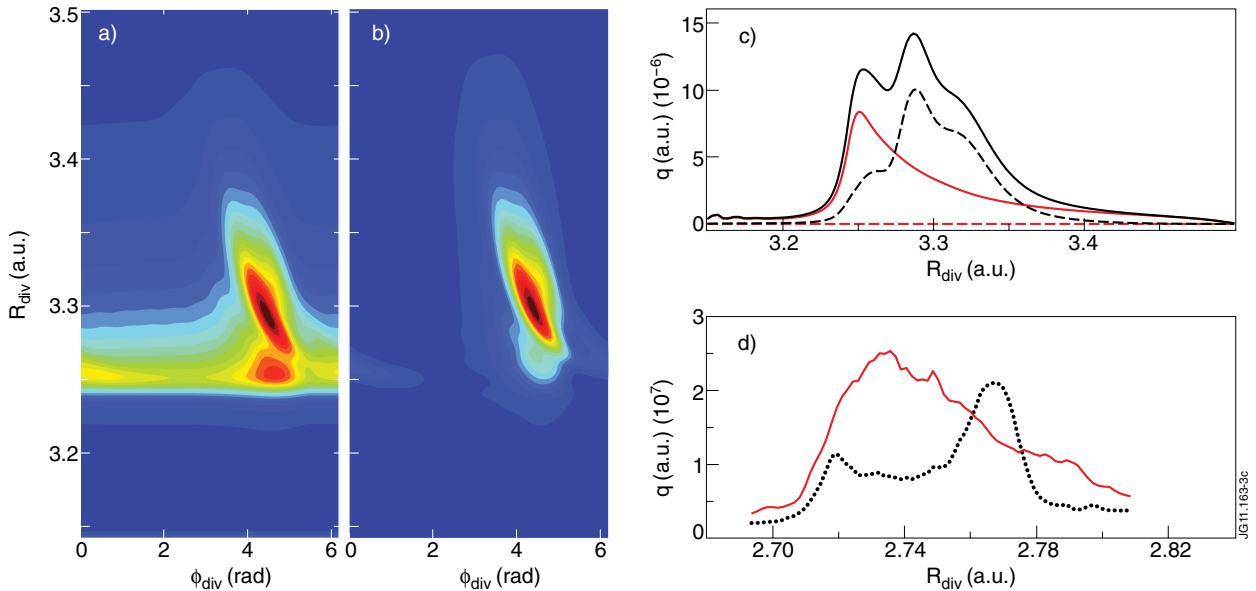


Figure 3: Heat flux density on the outer divertor target from JOREK simulation: a) Total deposition b) Asymmetric component. Pellet injection location is at $\Phi = 0$. c) Profiles of total deposition (solid) and asymmetric component (dashed) at toroidal position with minimum (red) and maximum (blue) asymmetric contribution. d) Deposition profile of individual ELMs averaged over $t = 0$ to $t = 0.4\text{ms}$ with $t = 0$ defined by the peak power deposition: Pellet induced ELM (black) and spontaneous predecessor (magenta)